Princeton Plasma Physics Laboratory

PPPL- 4284

PPPL- 4284

# Temperature Contours and Ghost-Surfaces for Chaotic Magnetic Fields

S.R. Hudson, J. Breslau

January 2008

Prepared for the U.S. Department of Energy under Contract DE-AC02-76CH03073.

# Princeton Plasma Physics Laboratory
# Report Disclaimers

---

## Full Legal Disclaimer



## Trademark Disclaimer



---

# PPPL Report Availability

## Princeton Plasma Physics Laboratory:

http://www.pppl.gov/techreports.cfm

## Office of Scientific and Technical Information (OSTI):

http://www.osti.gov/bridge

---

**Related Links:**

**U.S. Department of Energy**

**Office of Scientific and Technical Information**

**Fusion Links**

# Temperature contours and ghost-surfaces for chaotic magnetic fields

S.R. Hudson, J. Breslau
*Princeton Plasma Physics Laboratory, PO Box 451, Princeton NJ 08543.*
(Dated: January 22, 2008)

Steady state solutions for anisotropic heat transport in a chaotic magnetic field are determined numerically and compared to a set of "ghost-surfaces", surfaces constructed via an action-gradient flow between the minimax and minimizing periodic orbits. The ghost-surfaces are in remarkable agreement with the temperature contours.

A variety of transport processes in magnetically confined plasmas are dominated by strong *parallel* transport along the magnetic field $\mathbf{B}$, with small *perpendicular* transport. Coordinates adapted to the structure of the magnetic field, magnetic coordinates, therefore provide an elegant theoretical description of plasma dynamics and often enhance numerical accuracy. Magnetic coordinates are analogous to the action-angle coordinates of Hamiltonian systems and may be constructed globally when the magnetic field-lines lie on nested, invariant toroidal surfaces, ie. when the field is integrable. Integrable magnetic fields are however the exception rather than the rule. Error fields [1] or internal plasma motions, eg. microtearing instabilities [2], result in partially chaotic magnetic fields in tokamaks, and chaotic fields are intrinsic to the non-symmetric stellarator [3].

Here we present a coordinate framework adapted to the structure of *chaotic* magnetic fields, which we call chaotic magnetic coordinates, and show that this framework allows a simple description of anisotropic transport. We consider heat transport, as described by

$$\frac{\partial T}{\partial t} = \nabla \cdot \left(\kappa_\parallel \nabla_\parallel T + \kappa_\perp \nabla_\perp T\right) + Q, \qquad (1)$$

where $T$ is the temperature, $t$ is time, and $\kappa_\parallel$, $\kappa_\perp$ are the (constant) parallel and perpendicular diffusion coefficients. The parallel derivative, $\nabla_\parallel T$, is given $\nabla_\parallel T = \mathbf{b}\,\mathbf{b}\cdot\nabla T$, where $\mathbf{b} = \mathbf{B}/|B|$, and the perpendicular derivative is $\nabla_\perp T = \nabla T - \nabla_\parallel T$. The term $Q$ allows for heat sources/sinks, but we set this to zero and examine the non-trivial, steady state solutions forced by inhomogeneous boundary conditions.

For fusion plasmas, the ratio $\kappa_\parallel/\kappa_\perp$ may exceed $10^{10}$ [4]. Strong anisotropy has different consequences, depending on whether the magnetic field-lines lie on nested flux surfaces, whether the field is slightly chaotic, or whether the field is so chaotic that the motion of field-lines is effectively random. In the first case the temperature is a surface function, $T = T(\psi)$, where $\psi$ labels flux surfaces, and gradients can be supported. For the opposite case of *extreme* chaos, where the field-lines seem to wander randomly over a volume, the strong parallel transport results in temperature flattening, $T = const.$ It is the intermediate case of critical (near threshold) chaos that is most relevant for toroidal plasma confinement. The temperature is then dominated by the fractal structure of the chaotic magnetic field. How chaotic magnetic coordinates allow this structure to be understood is the topic of this letter.

A chaotic magnetic field is a fractal mix of (i) invariant flux (KAM) surfaces [5, 6], which are labeled by their irrational rotational-transform; (ii) cantori (broken KAM surfaces), in particular the near-critical cantori which present effective but *partial* barriers to field-line transport [7]; (iii) unstable periodic orbits and their unstable manifolds which constitute the stochastic sea; and (iv) stable periodic orbits and elliptic island chains [5, 6].

The complexity of the field structure dictates that Eq.(1) must be solved numerically [8, 9], but this is not an easy task. The temperature must be represented as a scalar field of three-dimensional space, $T = T(\psi, \theta, \phi)$, where $\theta, \phi$ are arbitrary poloidal and toroidal angles. The infinitely many irregular field-lines in the stochastic sea may come arbitrarily close to each other. For large $\kappa_\parallel$ the temperature along the field-lines is almost constant, and for small $\kappa_\perp$ the cross field interaction is very weak. The temperature becomes a fractal function of position as $\kappa_\parallel/\kappa_\perp$ increases and the resolution requirements become overwhelming. The challenge is to achieve sufficient accuracy to resolve the near-fractal structure, ensuring that numerical error, "numerical diffusion", does not overwhelm the small perpendicular diffusion.

It would be of great benefit if some theoretical insight allowed the representation of the temperature to be simplified. For example, on the KAM surfaces, we may expect that the temperature will be constant. We also know [4] that the temperature will flatten inside the island chains when the island width, $\Delta w$, exceeds a critical value, $\Delta w \sim (\kappa_\perp/\kappa_\parallel)^{1/4}$. Within the stochastic sea, it is tempting to conclude that the strong parallel transport results in a flat temperature profile, or that the transport is uniform. For near-threshold chaos however, this is an oversimplification. Irregular trajectories, with finite Lyapunov exponent, may take an impractically long time to sample the accessible volume. Attempts to determine transport by averaging [10] must take into account that within the stochastic sea there exists a finite volume of regular motion (the magnetic islands), and what the relative volume of irregular versus regular motion is remains an open question in non-linear dynamics. The point is, chaos is not random.

The key to understanding the structure of the temperature in the stochastic sea is to realize that the most

effective barriers to field-line transport are given by the cantori. Cantori are the invariant sets under the field-line flow remaining after a KAM surface has been destroyed by chaos [11–13], but they have an infinity of gaps where field-lines may leak through. In the near-critical case (when the level of chaos just exceeds that required to break the KAM surface) the gaps in the cantorus are small, and the field-line flux across the cantorus is small. As the most robust KAM surfaces have noble rotational-transform [14], the most important barriers to field-line transport in chaotic fields are usually the noble cantori. As the level of chaos increases, the gaps in the cantorus enlarge and the field-line flux increases: super-critical cantori have little effect on field-line transport.

So we have a situation in which regions of local temperature flattening are produced by the significant islands, between which the irrational barriers may support gradients. If coordinate surfaces can be constructed that coincide with the irrational barriers, then the temperature profile will approximate a smoothed devil's staircase [15]. Clearly, coordinate surfaces should coincide with any KAM surfaces that exist, but here we consider a region in which all KAM surfaces are destroyed and the most significant barriers are provided by the noble cantori. To construct a coordinate framework based on cantori we need to "close the gaps", and this can be done by constructing ghost-surfaces, as we now describe.

Cantori are approximated by high-order, action-minimizing periodic orbits [16]. These are conveniently found using the action formalism of magnetic-field-line dynamics [17]. The action formalism is also required for the construction of the ghost-surfaces, which are defined using the action-gradient flow. Magnetic field-lines are stationary curves $\mathcal{C}$ of the action integral [18],

$$S_{\mathcal{C}} = \int_{\mathcal{C}} \mathbf{A} \cdot \boldsymbol{dl}, \tag{2}$$

where $\mathbf{B} = \nabla \times \mathbf{A}$. We use a vector potential in canonical form $\mathbf{A} = \psi \nabla\theta - \chi \nabla\phi$, where $\chi(\psi, \theta, \phi)$ is the field-line Hamiltonian:

$$\chi = \psi^2/2 + \sum \chi_{m,n} \cos(m\theta - n\phi). \tag{3}$$

A piecewise-linear approximation for $\mathcal{C}$ is sufficient, where between $\phi \in [i\Delta\phi, (i+1)\Delta\phi]$ a "trial"-curve is given $\theta(\phi) = \theta_i + (\theta_{i+1} - \theta_i)(\phi - \phi_i)/\Delta\phi$ for $\Delta\phi = 2\pi q/N$, and $\psi = \dot{\theta}(\phi)$ [17]. We restrict attention to $(p, q)$ periodic curves, $\theta(\phi + 2\pi q) = \theta(\phi) + 2\pi p$, by constraining $\theta_N = \theta_0 + 2\pi p$. The action integral is now piecewise directly solvable and is a rapidly computable function of the $N$ independent parameters, $S(\theta_0, \theta_1, \ldots, \theta_{N-1})$. Periodic orbits are those particular trial-curves for which the action gradient, $\nabla S = (\partial S/\partial\theta_1, \partial S/\partial\theta_2, \ldots)^T$, is zero. Finding periodic orbits amounts to a multi-dimensional root find, and an $N$-dimensional Newton method is suitable. The derivative of the action gradient, the Hessian $D^2 S$, is a cyclic, tri-diagonal matrix of the second derivatives of $S$. The action extremizing approach allows both the stable (minimax) and unstable (minimizing) orbits to be quickly found, even for orbits with periodicities in the tens of thousands for strongly chaotic fields [17].

The Hessian at the minimax orbit generically has a single negative eigenvalue, and the associated eigenvector indicates the direction in configuration space along which the action integral decreases. Ghost-surfaces are constructed by pushing a trial-curve off the minimax orbit in this direction, then allowing the curve to evolve down the gradient flow:

$$\frac{d\theta_i}{d\tau} = -\frac{\partial S}{\partial \theta_i}, \tag{4}$$

where $\tau$ is any suitable integration parameter. As the action is decreasing under this flow, and the curves are constrained to be periodic, the trial-curve will evolve into the minimizing periodic orbit, and in doing so will trace out a surface, the ghost-surface of periodicity $(p, q)$.

Ghost-surfaces were originally introduced for the standard map [19, 20] (in this context, they are called ghost circles), and they were found to be non-intersecting: we have not found exceptions to this. Any selection of ghost-surfaces may form the framework of the chaotic coordinates, and by choosing rationals $p/q$ that approximate a given irrational we may consider *irrational* ghost-surfaces. To complete the chaotic coordinates, the surfaces can be interpolated radially to provide a continuous foliation of space, and a suitable angle coordinate can be imposed, for example so that each trial-curve comprising the ghost-surface is straight.

Intuition suggests that the irrational ghost-surfaces that close the gaps in near critical cantori would coincide with temperature iso-contours. What was unexpected is how closely the ghost-surfaces coincide for even the strongly super-critical cantori.

To compute steady state solutions of Eq.(1), a second-order finite-difference model is employed. The parallel and perpendicular diffusions are separated numerically [21] by locally introducing straight-field line (Clebsch) coordinates $(\alpha, \beta, \phi)$, where $\mathbf{B} = \nabla\alpha \times \nabla\beta$. The parallel diffusion operator becomes

$$\nabla_\parallel^2 T = B^\phi \frac{\partial}{\partial \phi} \left( \frac{B^\phi}{B^2} \frac{\partial T}{\partial \phi} \right), \tag{5}$$

where the partial derivative with respect to $\phi$ is along a magnetic field line: for each grid point $(\psi_{i,j}, \theta_{i,j})$ on the plane $\phi_k = k\Delta\phi$, with temperature $T_{i,j,k}$, the parallel gradient on the *forward* "half-$\phi$" grid is approximated

$$\left.\frac{\partial T}{\partial \phi}\right|_{i,j,k+1/2} = \frac{T(\psi, \theta, \phi_{k+1}) - T_{i,j,k}}{\Delta\phi}, \tag{6}$$

where $(\psi, \theta, \phi_{k+1})$ is where the field-line starting from $(\psi_{i,j}, \theta_{i,j}, \phi_k)$ intersects the $\phi_{k+1}$ plane, which can always be determined by field line tracing. In general, this point will not coincide with a grid point, so bi-linear interpolation is used to estimate $T(\psi, \theta, \phi_{k+1})$. The quantity

$\partial_\phi T|_{i,j,k-1/2}$ on the *backward* half-$\phi$ grid is defined similarly. The first partial $\phi$-derivatives on the $k+\frac{1}{2}$ and $k-\frac{1}{2}$ half-grids are combined, along with the factors $B^\phi$ and $B^2$, to give a centered, finite-difference realization of the second-order, parallel-diffusion operator.

For $\kappa_\parallel \gg \kappa_\perp$, the temperature will vary weakly along magnetic field-lines. So, $\Delta\phi$ need not be small. We choose $\Delta\phi = 2\pi$ and perform the computation on a single plane. This reduces the computational burden and allows additional resolution within the plane, ie. in the perpendicular direction, which is required to resolve the small scale of the solution for small $\kappa_\perp$.

The diffusion perpendicular to $\mathbf{B}$ is approximated by a diffusion instead perpendicular to $\phi$. This approximation introduces a negligible error when the field is dominantly toroidal and when $\kappa_\perp/\kappa_\parallel$ is small, and eliminates the need to compute the metric elements of the $(\alpha,\beta,\phi)$ coordinates, which in principle are determined from differentiating the field-line integration (ie. constructing the tangent map). The diffusive operator perpendicular to $\phi$ is given by the Laplacian

$$\nabla_\perp^2 T = \sqrt{g}^{-1}\left[\partial_\psi(\sqrt{g}T^\psi) + \partial_\theta(\sqrt{g}T^\theta)\right], \qquad (7)$$

where $T^\psi = g^{\psi\psi}T_\psi + g^{\psi\theta}T_\theta$ and $T^\theta = g^{\theta\psi}T_\psi + g^{\theta\theta}T_\theta$, where $T_\psi = \partial T/\partial\psi$ and $T_\theta = \partial T/\partial\theta$, and the geometric information is encapsulated in the 'raising' metric elements $g^{ab} = \nabla a\cdot\nabla b$ and the Jacobian, $\sqrt{g}$. The Laplacian is discretized using second-order finite differences [22].

The steady state condition,

$$\kappa_\parallel\nabla_\parallel^2 T + \kappa_\perp\nabla_\perp^2 T = 0, \qquad (8)$$

becomes a sparse linear system which is solved using an iterative Krylov method (Bi-CGStab [23]). We consider the region between two magnetic islands, namely the $(p,q) = (1,2),(2,3)$ islands at $\psi = \frac{1}{2}$ and $\psi = \frac{2}{3}$ respectively, which are excited by the $\chi_{2,1}$ and $\chi_{3,2}$ perturbation harmonics in Eq.(3), and we set $2\chi_{2,1} = 3\chi_{3,2} = k$, where $k$ is a perturbation parameter. The symmetry of the field allows $T(\psi,-\theta) = T(\psi,\theta)$, so a regular grid in $\psi,\theta$ is constructed in the region $\psi\in[\psi_l,\psi_u]$ and $\theta\in[0,\pi]$, where $\psi_l = 0.50$ and $\psi_u = 0.68$, with grid spacing $\Delta\psi = (\psi_u-\psi_l)/N$, $\Delta\theta = 2\pi/N$, where $N$ is the grid resolution. It is the chaotic structure of the field that is relevant to the present study, rather than geometry, so we use the simple Cartesian metric, $g^{\psi\psi} = g^{\theta\theta} = 1$, $g^{\psi\theta} = 0$, and $\sqrt{g} = 1$. The most robust KAM surface in this region appears to be the $\iota = 0.5607..$ surface, which has a critical perturbation $k = 2.039\times10^{-3}$ [17], so here we set the perturbation $k = 2.100\times10^{-3}$ to just exceed this critical value to give a field with connected chaos between the $(1,2)$ and $(2,3)$ islands. A Poincaré plot of this field is shown in Fig.1. The boundary conditions are $T(\psi,\theta) = 1$ for $\psi\le\psi_l$, and $T(\psi,\theta) = 0$ for $\psi\ge\psi_u$. We have confirmed the second order scaling of the error with respect to grid size, $e\sim\mathcal{O}(N^{-2})$, and the expected scaling of the critical island width $\Delta w\sim(\kappa_\perp/\kappa_\parallel)^{1/4}$. Temperature iso-contours are shown in Fig.1 for the case $\kappa_\perp/\kappa_\parallel = 10^{-10}$, with $N = 2^{12}$.

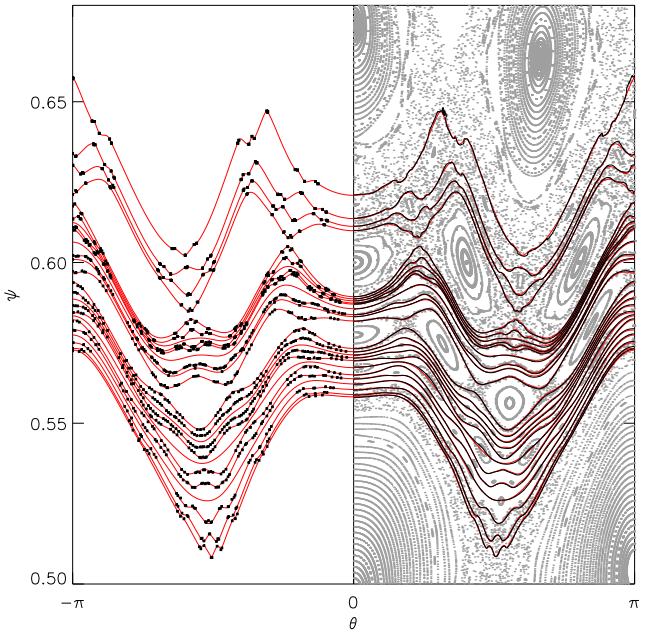


FIG. 1: (Color online) For $\theta < 0$ : The selected ghost curves (red lines) and cantori (black square dots). For $\theta > 0$ : Poincaré plot (gray dots), ghost curves (red lines) and the temperature contours (black lines) for $\kappa_\perp/\kappa_\parallel = 10^{-10}$.

There is a countable infinity of ghost-surfaces that may be selected: the optimal selection is determined by the island widths and $\kappa_\perp/\kappa_\parallel$. (An island width is not well defined when the separatrix becomes chaotic, but one could instead consider the resonance area [24].) We distinguish three types of surface: (i) low-order surfaces; (ii) high-order surfaces where $p/q$ approximates a noble irrational; and (iii) high-order surfaces where $p/q$ approximates a boundary irrational (an irrational that lies close to a low order rational [25]). When $\kappa_\perp$ is comparatively large, the fine scale structure of the field is overlooked and the low order islands have the dominant effect on the solution: in this case, a selection of low-order surfaces is suitable. As $\kappa_\perp$ is decreased, the temperature flattens across the larger islands, and the iso-contours will coincide with noble surfaces. As $\kappa_\perp$ is further decreased, the temperature adapts more closely to the separatrix structure of the island chains, and the boundary surfaces become relevant. In Fig.1 is shown a selection of ghost-surfaces. The ghost-surfaces bear a remarkable coincidence with level surfaces of the temperature: on this scale, the ghost-surfaces and iso-contours are nearly indistinguishable.

For the irrational surfaces, minimizing periodic orbits that approximate the associated cantori are shown. For the super-critical cantori the dots cluster together [26] and large gaps emerge; however, the agreement between the super-critical ghost-surfaces (eg. the top four surfaces

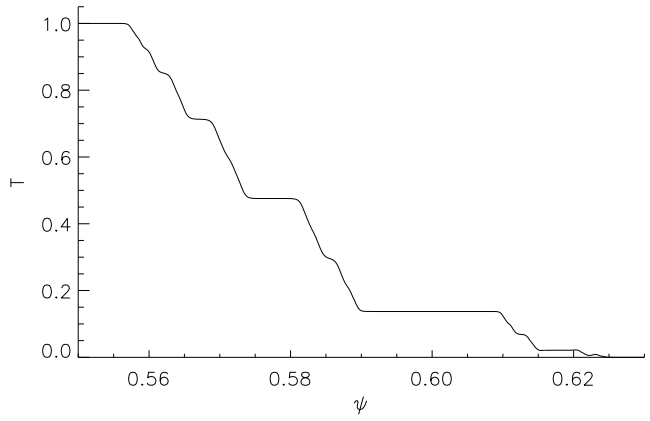


FIG. 2: Temperature profile for case shown in Fig.1.

in Fig.1) and the iso-contours is excellent. The temperature profile Fig.2 along the symmetry line $\theta = 0$ reveals the structure of the solution: across the larger islands (rational zones) the temperature flattens, and across the cantori and small islands (irrational zones) temperature gradients are supported. Even though no KAM surfaces exist, the heat flux required to sustain the imposed temperature gradient is enhanced only by a factor of two compared to the integrable case: the irrational barriers are quite capable of supporting temperature gradients even in chaotic fields.

Given an optimal selection of ghost-surfaces, labeled by $s$, the temperature may be written in chaotic coordinates as $T = T_o(s) + \delta T(s, \theta, \phi)$, where $T_o(s)$ is generally a smoothed devil's staircase, and $\delta T$ is small compared to $T_o$ for small $\kappa_\perp/\kappa_\parallel$. Such an expression may serve as the basis for simplified theoretical and numerical descriptions of heat transport in chaotic fields. The parallel diffusion gives a relaxation that is dominantly tangential to the ghost-surfaces, which are "almost-invariant" under the field line flow. Future work will explore whether ghost-surfaces are optimal in this respect, or whether other almost-invariant surfaces [27] are preferable. This work was supported in part by U.S. Department of Energy Contract No. DE-AC02-76CH03073 and Grant No. DE-FG02-99ER54546.

[1] T. E. Evans, R. A. Moyer, P. R. Thomas, J. G.Watkins, T. H. Osborne, J. A. Boedo, E. J. Doyle, M. E. Fenstermacher, K. H. Finken, R. J. Groebner, et al., Phys. Rev. Lett. **92**, 235003 (2004).
[2] K. L. Wong, S. Kaye, D. R. Mikkelsen, J. A. Krommes, K. Hill, R.Bell, and B. LeBlanc, Phys. Rev. Lett. **99**, 135003 (2007).
[3] S. R. Hudson, M. J. Hole, and R. L. Dewar, Phys. Plasmas **14**, 052505 (2007).
[4] R. Fitzpatrick, Phys. Plasmas **2**, 825 (1995).
[5] A. J. Lichtenberg and M. A. Lieberman, *Regular and Chaotic Dynamics, 2nd ed.* (Springer-Verlag, New York, 1992).
[6] J. D. Meiss, Rev. Mod. Phys. **64**, 795 (1992).
[7] R. S. MacKay, J. D. Meiss, and I. C. Percival, Phys. Rev. Lett. **52**, 697 (1984).
[8] C. R. Sovinec, T. A. Gianakon, E. D. Held, S. E. Kruger, and D. D. Schnack, Phys. Plasmas **10**, 1727 (2003).
[9] L. E. Sugiyama, W. Park, H. R. Strauss, S. R. Hudson, D. Stutman, and X.-Z. Tang, Nucl. Fus. **41**, 739 (2001),
[10] A. B. Rechester and M. N. Rosenbluth, Phys. Rev. Lett. **40**, 38 (1978).
[11] I. C. Percival, in *Nonlinear Dynamics and the Beam-Beam interaction*, edited by M. Month and J. C. Herra (AIP, New York, 1979), vol. 57 of *AIP Conf. Proc.*
[12] S. Aubry and P. Y. Le Daeron, Physica D **13**, 381 (1983).
[13] J. N. Mather, Topology **21**, 457 (1982).
[14] J. M. Greene, J. Math. Phys. **20**, 1183 (1979).
[15] S. R. Hudson, Phys. Rev. E. **75**, 046211 (2007).
[16] H. J. Schellnhuber, H. Urbschat, and A. Block, Phys. Rev. A. **33**, 2856 (1986).
[17] S. R. Hudson, Phys. Rev. E. **74**, 056203 (2006).
[18] J. R. Cary and R. G. Littlejohn, Ann. Phys. **151**, 1 (1983).
[19] C. Golé, J. Differ. Equations **97**, 140 (1992).
[20] R. S. MacKay and M. R. Muldoon, Phys. Lett. A **178**, 245 (1993).
[21] A.M.Runov, D.Reiter, S.V.Kasilov, M.F.Heyn, and W.Kernbichler, Phys. Plasmas **3**, 2132 (2001).
[22] S. Günter, Q. Yu, J. Krüger, and K. Lackner, J. Comp. Phys. **209**, 354 (2005).
[23] H. van der Vorst, *Iterative Krylov Methods for Large Linear Systems* (Cambridge University Press, 2003).
[24] R. S. MacKay, J. D. Meiss, and I. C. Percival, Physica D **27**, 1 (1987).
[25] J. M. Greene, R. S. MacKay, and J. Stark, Physica D **21**, 267 (1986).
[26] W. Li and P. Bak, Phys. Rev. Lett. **57**, 655 (1986).
[27] R. L. Dewar, S. R. Hudson, and P. Price, Phys. Lett. A **194**, 49 (1994).

The Princeton Plasma Physics Laboratory is operated
by Princeton University under contract
with the U.S. Department of Energy.

Information Services
Princeton Plasma Physics Laboratory
P.O. Box 451
Princeton, NJ 08543

Phone: 609-243-2750
Fax: 609-243-2751
e-mail: pppl_info@pppl.gov
Internet Address: http://www.pppl.gov